Available online at www.sciencedirect.com
SCIENCE DIRECT®
Journal of Molecular Catalysis A: Chemical 228 (2005) 151–162
JOURNAL OF MOLECULAR CATALYSIS A: CHEMICAL
www.elsevier.com/locate/molcata

X-ray photoelectron spectroscopy studies of laterite standard reference material

J. Mendialdua[a], R. Casanova[a,*], F. Rueda[a], A. Rodríguez[a], J. Quiñones[a], L. Alarcón[a], E. Escalante[a], P. Hoffmann[a], I. Taebi[b], L. Jalowiecki[b]

[a] *Laboratorio de Física de Superficies. Dpto de Física. Fac. de Ciencias, ULA. Mérida 5101, Venezuela*
[b] *Laboratoire de Catalyse Héterogène, U.R.A.C.N.R.S. No 402, Universite des sciences et Techniques de lille Flandres-Artois, 59655 Villeneuve d'Ascq Cedex, France*

Available online 26 November 2004

Abstract

X-ray photoelectron spectroscopy is used to characterize two natural samples of laterite standard reference materials (certified geologically), a mechanical mixture of Fe_2O_3, SiO_2, and Al_2O_3 in a 4:2:1 proportion. Fe_2O_3, SiO_2, and Al_2O_3 samples were also analyzed for comparison purposes. Special attention was paid to peak shape, FWHM, comparison of the same XPS peaks of different samples, and peak shifts. The XPS results reveal the presence of some kind of iron aluminate prevailing on the surface of the laterite standard reference materials. It is also observed that the mechanical mixture exhibits a differential charging effect. Our report provides important information for the researchers doing XPS on these materials when they are used in catalytic reactions.

Keywords: XPS; Laterites; Oxygen; Auger parameter; Iron

1. Introduction

Our laboratory has dedicated some effort to study catalytic materials suitable for several technological processes. One of these materials are laterites [1] which are used in the oil industry as catalysts for hydrocracking and HDM (hydrodemetallization) processes [2,3], as well as in the metallurgical industry as aluminum, iron and nickel ores. To characterize a given catalyst, it is very important to determine its surface composition and XPS is one of the most appropriate analytical techniques used today. A cooperative programme [4,5] with some laboratories abroad allows us to perform both surface and bulk characterization of these materials. So far, we have studied a series of natural laterites not standardized geologically whose reported bulk composition is, besides other minor species, X% SiO_2, Y% Fe_2O_3, Z% Al_2O_3 where Y is greater than 20, with $Z = 0$ in one extreme of this series [6,7], and two samples [7,8] with $X \approx 1$% in the other extreme. Because of the technological and economic importance of laterites, the Working Group of the International Geological Correlation Programme (project IGCP-129 sponsored by UNESCO) prepared a set of laterite standard reference materials with different iron, aluminum and silica contents. In previous work [6,7] we presented evidence confirming that the lateritic material surface is not a simple oxide mixture, but consists mainly of iron aluminates and aluminosilicates, contrary to literature reports [1,9,10] on laterite bulk characterization. These results prompted the study of two samples (named VL1 and SLB1) of laterite standard reference materials [11,12] which were treated similarly and compared their behaviour, under oxidation and reduction treatments (due to their use in catalytic reactions which involve these processes), with that of Fe_2O_3, SiO_2, and Al_2O_3 samples treated similarly, and that of a sample obtained from a mechanical mixture of these oxides in a 4:2:1 proportion, in order to mimic the LV5 laterite previously studied [7], which lies in the middle of the series mentioned above. The ultrapure powder oxides employed were analyzed separately. Here, we report the sample characterization by X-ray photoelectron spectroscopy (XPS).

* Corresponding author. Tel.: +58 2742401286/58 2742401339.
E-mail address: rodrigoc@ula.ve (R. Casanova).

1381-1169/$ – see front matter © 2004 Elsevier B.V. All rights reserved.
doi:10.1016/j.molcata.2004.09.040

2. Experimental details

2.1. Samples

The reported weight composition [11] of the VL1sample was: 37.38% Al_2O_3, 35.77% Fe_2O_3, 1.16% SiO_2, 3.15% TiO_2 and lost on ignition (LOI) 22.54%. It was extracted from the Serranía de Los Guaicas, west of Canaima, 230 km south of Ciudad Bolivar, Venezuela. The SLB1 sample has a weight composition [12] of: 45.5% Al_2O_3, 24.03% Fe_2O_3, 1.93% SiO_2, 1.75% TiO_2 and LOI 26.79%. It was extracted from the western part of Suriname in the Bakhuis Mountains.

The mechanical mixture (MMLV5) has a weight composition of: 57.14% Fe_2O_3, 28.57% SiO_2 and 14.29% Al_2O_3.

The samples were analyzed before (BT) and after (AT) being used in catalytic tests [13] in oxidative dehydrogenation of propane to propene ($C_3H_8 + 1/2\ O_2 \rightarrow C_3H_6 + H_2O$); the latter samples were translated to the XPS spectrometer exposing them to atmospheric conditions. To perform the catalytic test the samples were previously calcinated at 500 °C. The reaction took place in a fixed bed stainless steel reactor. The samples were analyzed in the temperature range from 250 to 500 °C. The reactants composition was 5% C_3H_8, 15% O_2 and 80% N_2, and the total flow was 6 l.n.h^{-1}; the catalyst mass used was 1 g.

2.2. XPS measurements

XPS measurements were carried out in a LHS 10S spectrometer (University of Lille I, France) and its specifications have been reported previously [7,14] and a VSW spectrometer (Universidad de los Andes, Merida, Venezuela) with a sample treatment chamber and Ar^+ ion etching facilities, spectrometer vacuum was in the low 10^{-8} mbar range and its hemispherical analyzer (100 mm mean radius) was operated at 22.4 eV constant pass energy. The Leybold spectrometer energy scale was calibrated using the following phoelectron peak positions: Au $4f_{7/2}$, Ag $3d_{5/2}$, Cu LMM, Cu $2p_{3/2}$, Ag LMM, while for the VSW spectrometer the levels: Ag $3d_{5/2}$, Au $4f_{7/2}$, Cu $2p_{3/2}$, Cu LMM and the Ni Fermi edge were used for the Mg and Al anodes. Average time taken to record a XPS spectrum was near 5 min. Special attention was paid to the C 1s line of adventitious carbon to monitor contamination from the background vacuum. Non-monochromatic Al Kα radiation (1486.6 eV) was used as the X-ray source with 300 W constant power.

The reduction of the samples surface was achieved by annealing and Ar^+ etching and/or exposure to H_2 depending on the spectrometer used. In the Leybold spectrometer the samples were treated thus:

(1) Ar^+ ion etching for 60 min with 3 kev ions.
(2) Thermal treatment in vacuum at 773 K for 14 h. We have verified that, in our case, the order of the reduction treatments is not important.
(3) Re-oxidation in an oxygen atmosphere at 773 K.

In the VSW spectrometer, samples were treated likewise, in addition to a reduction treatment in 10^{-4} mbar of H_2 at 773 K during 4–20 h depending on the sample. XPS spectra were taken before and after each sample treatment. Due to their hygroscopic nature, all the samples (excepting BT VL1, BT SLB1, SiO_2, and Al_2O_3) analysed in this report were heated at 423 K before introducing them into the analysis chamber in order to preserve its vacuum. For this reason, BT VL1, BT SLB1, samples were calcined due to the high content of interstitial water; SiO_2 and Al_2O_3 were also calcined before XPS analysis.

The 285.0 eV C 1s binding energy of adventitious carbon was used, whenever possible, as an acceptable binding energy reference; however, when this peak intensity was very low, the Al 2p binding energy in Al_2O_3 (74.6 eV) or the Si 2p binding energy in SiO_2 (103.8 eV) were used as internal energy references depending on the sample under study, since it has been shown [8] that these two oxides are very stable under reduction treatments more severe than those used here; however, Fe_2O_3 does experience transformations; in this case we have found that O 1s at 530. 3 eV [15] is a better energy reference than C 1s of adventitious carbon. The MMLV5 sample exhibited a differential charging effect [16,17], which introduced inaccuracies on determining the binding energies. In this study, special attention was paid to peak shape, FWHM, etc., to facilitate reaching conclusions from the XPS results. The raw spectra for this report attained a very good signal to noise ratio and were smoothed by using a Fourier transform routine after background subtraction according to the Shirley method [18].

$K\alpha_{3,4}$ X-ray satellite peaks were removed by a software routine developed at the University of Lille-France by J.C. Marshal. The possible effects on the quality of XPS spectra have been reported by Mendialdua [19]. The photoelectron peaks were fitted by a procedure based on the variation of parameters such as peak position, width, and height. Each sample was impregnated with ultra pure isopropanol to prepare a suspension that was deposited on a stainless steel sample holder. The sample was dried before being introduced into the preparation chamber where it was heated at 373 K for 15 min. Good adherence and uniformity of the sample was found with this method of sample mounting, as reported in previous studies [6].

3. Results and discussion

It is expected that the presence of oxides as the main constituents in the studied laterites should be reflected in similar responses under the same sample treatments as the individual oxides and the mechanical mixture. In what follows, we present the XPS results corresponding to the behaviour of the samples studied in this report under oxidation and reduction treatments. In the discussion, special attention is paid to peak shape, FWHM, peak shifts and comparison among same XPS peaks of different samples;

Table 1
Electron binding energies (eV) of the core levels O 1s, Fe $2p_{3/2}$, Al 2p, Al 2s, Si 2p and Si 2s in Al_2O_3, Fe_2O_3, Si O_2 and VL1 after several sample treatments

Sample condition	O 1s, E_b (eV) ± 0.1	Fe $2p_{3/2}$, E_b (eV) ± 0.2	Al 2p, E_b (eV) ± 0.1	Al 2s, E_b (eV) ± 0.1	Si 2p, E_b (eV) ± 0.1	Si 2s, E_b (eV) ± 0.1
Al_2O_3						
Calcined	531.3		74.6	119.4		
H_2 reduced	531.1		74.6	119.3		
Ion etched	531.2		74.6	119.4		
Re-oxidized	531.2		74.6	119.7		
Fe_2O_3						
AR	530.3	711.4				
Calcined	530.3	711.1				
Ion etched	530.3	711.1				
H_2 reduced	530.3	711.1				
Re-oxidized	530.3	710.9				
SiO_2						
Calcined	532.7				103.8	154.7
H_2 reduced	533. 0				103.8	154.7
Ion etched	532.8				103.8	154.8
Re-oxidized	533.0				103.8	154.8
VL1						
BT						
Oxidized	532.2		74.4	119.3		
	530.3	711.8				
Ion etched	532.1		74.3	118.3		
	530.3	711.3				
Annealed	531.0		74.0	118.5		
	529.4	710.0				
Re-oxidized	532.2		74.4	119.3		
	530.4	712.0				
AT						
AR	532.0		74.2	119.1		
	530.1	711.4				
Annealed	532.0		74.5	119.6		
	530.1	711.3				
Ion etched	532.1		74.5	119.4		
	530.3	711.1				
Re-oxidized	532.1		74.3	119.2		
	530.4	711.7				

for this, we analysed the O 1s, Fe 2p, Al 2p and Si 2p atomic levels corresponding to the elements present in these samples.

3.1. SiO_2

In this sample, the binding energy of Si 2p (103.8 eV) was taken as an internal binding energy reference; good agreement with the C 1s (285.0 eV) reference was found. Binding energy values for this sample are shown in Table 1. The Si 2p level did not show appreciable modification, except after Ar^+ etching when a FWHM increase by ≈0.3 eV occurs which is maintained during the sample reoxidation, in agreement with previous results [20].

The O 1s peak shifts by 0.3 eV to higher binding energy under hydrogen reduction without any peak shape or FWHM changes; during Ar sputtering the peak FWHM increases slightly accompanied by a 0.2 eV shift to lower binding energies. During re-oxidation the O 1s peak shifts by 0.2 eV to higher binding energy probably due to the presence of some water in the oxygen gas used; but the peak width before sputtering is not recovered.

3.2. Al_2O_3

Binding energy values for this sample, using Al 2p (74.6 eV) as energy reference are listed in Table 1, the C 1s level was used also as reference, for comparison purposes, when peak intensity allowed it (values not shown). Energy differences of the order of 0.3 eV were obtained for the binding energy values given by using the above energy references.

O 1s binding energy decreases by 0.2 eV without FWHM modification after H_2 reduction; with ion bombardment there is a 0.1 eV binding energy increase and its width diminishes slightly; with re-oxidation the binding energy do not change and peak width is slightly smaller than after ion etching.

3.3. Fe_2O_3

Binding energies for this sample were corrected employing the O 1s (530.3 eV) binding energy; using the C 1s (285.0 eV) energy reference does not give good agreement especially for some sample treatments. The energy difference between the charge effects using the C 1s reference and the O 1s reference is 0.5 eV for the sample as received (AR); 0.1 eV both for the calcined and ion etched sample. After H_2 reduction (for 4 h; 10^{-4} mbar), the charge effect using the C 1s reference is −0.4 eV and using the O 1s reference is +0.4 eV. This shows that the C 1s reference is not suitable for this sample. In fact, after re-oxidation the charge effects are both positive and the energy difference between them is 0.7 eV.

O 1s peak for the Fe_2O_3 sample in the as received condition (AR) has two components: one related to oxygen bonded to iron and the other attributed to OH. During sample calcination the OH component increases (probably due to H_2O contamination) and an oxygen species appears about 528 eV; we do not have yet a satisfactory explanation for the appearance of this species; it seems related to an excess of oxygen (sample calcination and reoxidation) present on the sample surface and is not likely due to differential charge effects if one takes into account the sample homogeneity and the fact that the oxygen sample treatments (calcination and reoxidation) are less likely to produce such effects in a sample like Fe_2O_3. After ion bombardment peak width is maintained, while the oxygen species at 528 eV disappears; with H_2 reduction O 1s peak width increases due to an increase of the OH oxygen component; sample re-oxidation maintains the OH component and the 528 eV species reappears.

With calcination the Fe 2p level remains unchanged except for a very slight contribution near 708 eV; the intensity of this component (≈708 eV) and Fe 2p peak width increases while the satellite structure loses definition with ion bombardment; H_2 reduction increases the effects observed on the ion etched sample, and a shift to lower binding energies is observed; re-oxidation does not recover the spectrum of the sample as received but rather that of the calcined sample.

4. SLB1 sample

The XPS spectra for Fe 2p, O 1s and Al 2p levels of this sample are presented in Figs. 1–3. A comparison of Fe 2p peaks of this sample (Fig. 1a–d) with those of Fe_2O_3 (Fig. 1e and f) is established; O 1s XPS peak for (BT) SLB1 sample after oxidation (Fig. 4a) is compared to the corresponding peak in Al_2O_3 (Fig. 4b) and Fe_2O_3 (Fig. 4c). Binding energy values for the different levels of this sample, referenced to the C 1s line, are given in Table 2. Al 2p levels (Fig. 3a–d) do not exhibit changes with either in shape or in width; but only in their binding energy. However, E_k (Al 2p) − E_k (O 1s) differences (independent of the charge effect) remain practically constant (see Table 3); which leads us to conclude that the Al 2p (74.6 eV) could also be taken as a good internal binding energy reference for this sample. In Table 4, the ra-

Table 2
Electron binding energies (eV) of the core levels O 1s, Fe $2p_{3/2}$, Al 2p, Al 2s, Si 2p and Si 2s in samples SLB1 and mixture M after sample treatments

Sample	O 1s, E_b (eV) ± 0.1	Fe $2p_{3/2}$, E_b (eV) ± 0.2	Al 2p, E_b (eV) ± 0.1	Al 2s, E_b (eV) ± 0.1	Si 2p, E_b (eV) ± 0.1	Si 2s, E_b (eV) ± 0.1
SLB1						
BT						
Oxidized	531.1	711.5	74.3	119.2		
Annealed	531.4	711.5	74.5	119.6		
Ion etched	531.7	711.2	74.8	119.7		
Re-oxidized	531.2	711.7	74.3	119.2		
AT						
AR	531.0	711.6	74.2	118.9		
Ion etched	531.3	711.1	74.5	119.2		
Annealed	531.0	710.8	74.2	118.9		
Re-oxidized	530.9	711.8	74.0	118.9		
Mixture M	*	*	*	*	*	*
AR	533.1				103.9	154.8
	531.6		75.0	119.8		
	529.4	710.3				
Calcined	532.5				103.1	154.0
	530.9		74.5	119.1		
	528.7	709.6				
H_2 reduced	533.9				104.5	155.6
	532.4		75.8	120.5		
	530.4	710.6				
Re-oxidized	533.3				103.0	153.9
	531.8		74.3	119.2		
	529.9	709.7				

*Values given without correcting the differential charge effect.

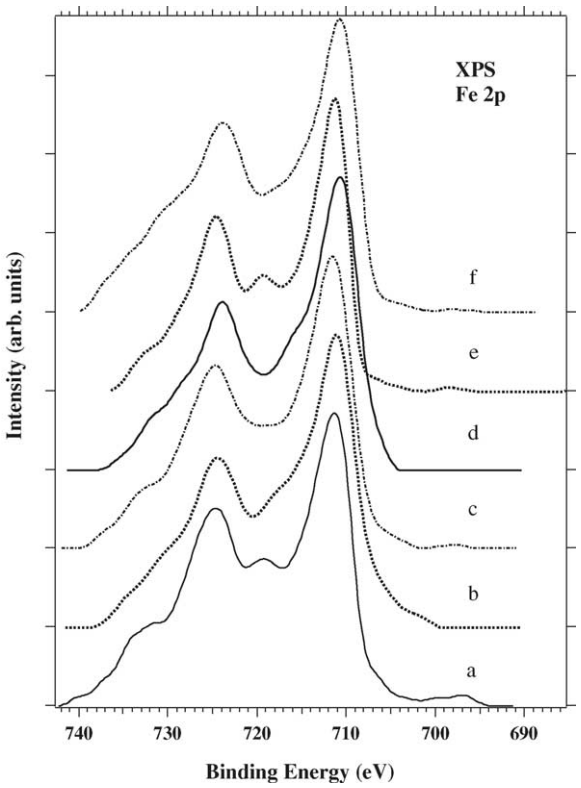

Fig. 1. Fe 2p XPS peaks of sample SLB1 under several conditions: (a) SLB1 before catalytic tests (BT) after an oxidation treatment; (b) SLB1 (BT) annealed and Ar^+ ion etched; (c) SLB1 after catalytic tests (AT) in the as-received condition; (d) SLB1 AT Ar^+ ion etched and thermal annealed, are compared to those of sample Fe_2O_3 in the (e) as received condition and (f) after a H_2 reduction treatment.

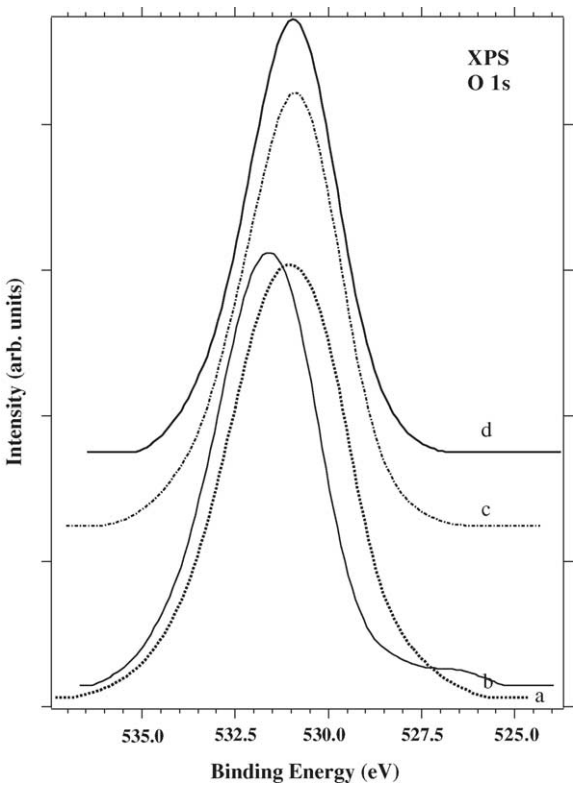

Fig. 2. O 1s spectral region of sample SLB1 for the conditions: (a) SLB1 before catalytic tests (BT) after an oxidation treatment; (b) SLB1 (BT) annealed and Ar^+ ion etched; (c) SLB1 after catalytic tests (AT) in the as-received condition; (d) SLB1 AT Ar^+ ion etched and thermal annealed.

tios of the surface atomic concentrations, obtained from our XPS data, are compared with our calculated bulk atomic ratios obtained from the reported weight composition of this sample (12). An Al enrichment with respect to the volume composition is observed.

4.1. Fe 2p level

In the BT SLB1 sample, heating for 12 h at 300 °C in vacuum produces minor changes on the Fe 2p peak (spectrum not shown); the satellites between Fe $2p_{1/2}$ and Fe $2p_{3/2}$ (inter peak satellite) peaks are not well resolved; the peak FWHM of Fe $2p_{3/2}$ increases slightly and a small contribution near $E_b \approx 708$ eV appears. Ar^+ etching increases FWHM slightly, and the intensity of species at $E_b \approx 708$ eV (see Fig. 1b); the satellite structure between the Fe 2p levels changes drastically (see Fig. 1a and b). Fe $2p_{3/2}$ peak width and intensity of species with $E_b < 710$ eV decrease with re-oxidation, and there is also a 0.6 eV peak shift to higher binding energies and the interpeak satellite is well defined; XPS spectrum of the re-oxidized BT SLB1 sample is similar to that of the re-oxidized AT sample (see Fig. 11d), with a better definition of satellite structure. Fe 2p XPS spectrum of the AT SLB1 sample (Fig. 1c) as received is very similar to that of the heated BT SLB1 sample (spectrum not shown); but the satellite structure between the Fe 2p levels does not show up. Ion etching causes broadening, and a contribution of species with $E_b < 709$ eV and a 0.5 eV shift to lower binding energies. Sample heating produces a more pronounced shift to lower binding energies, and the contribution of species with $E_b < 709$ eV is marked (see Fig. 1d). Sample re-oxidation of AT SLB1 causes a decrease in the FWHM and in the contribution of species with $E_b < 709$ eV, and a reappearance of the interpeak satellite structure (Fig. 11d). The whole of this is coherent with a certain degree of iron reduction during annealing and ion etching and a sample reoxidation once it is in contact with oxygen.

4.2. O 1s level

This peak, in both BT SLB1 and AT SLB1 samples looks very symmetric (Fig. 2), which makes peak decomposition into several components tricky, since its width, that could be greater than 3.25 eV, points to their presence. In the BT SLB1 sample, FWHM varies between 3.05 eV (re-oxidized) and 3.65 eV (oxidized) (Fig. 2a), and in the AT SLB1 sample the width varies between 2.8 eV (re-oxidized) (Fig. 8g), and 3eV (sample as received) (Fig. 2c); peak asymmetry present

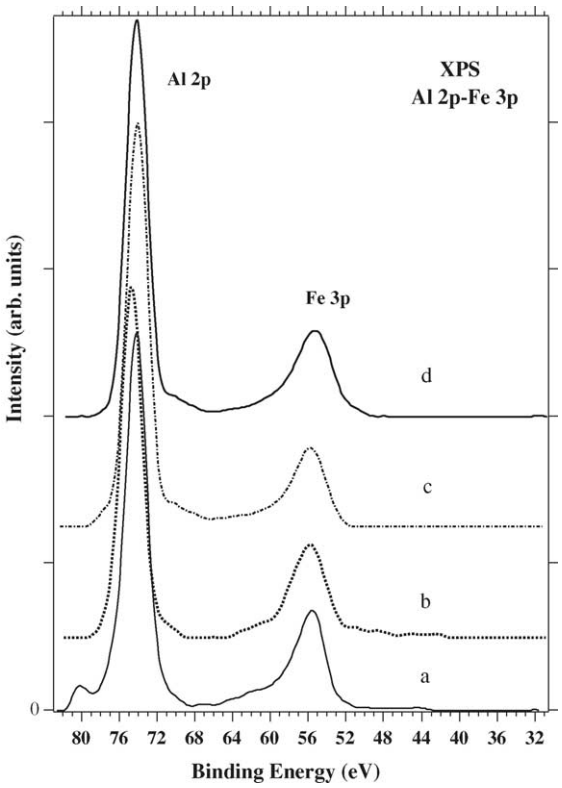

Fig. 3. Al 2p XPS spectra for: (a) SLB1 before catalytic tests (BT) after an oxidation treatment; (b) SLB1 (BT) annealed and Ar^+ ion etched; (c) SLB1 after catalytic tests (AT) in the as-received condition; (d) SLB1 AT Ar^+ ion etched and thermal annealed.

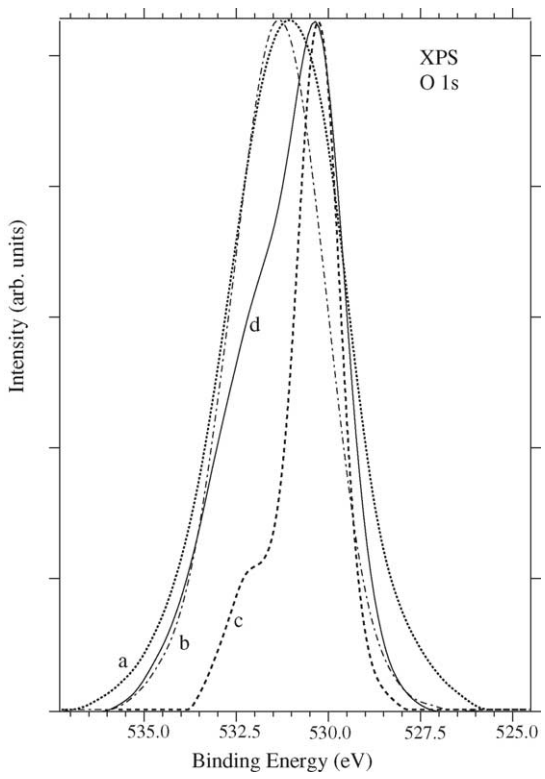

Fig. 4. The O 1s XPS region for samples: (a) SLB1 BT after an oxidation treatment; (b) Al_2O_3 after a calcination process; (c) Fe_2O_3 in the as-received condition; (d) VL1 BT after an oxidation treatment.

is exhibited by the two re-oxidized samples, when it reaches 0.35 eV to higher binding energies.

The O 1s peak in BT SLB1 annealed sample (spectrum not shown) shows a ≈0.5 eV shift to higher binding energies, and a pronounced FWHM reduction, due to intensity reduction of species with $E_b < 530$ eV. Ion bombardment causes a ≈0.3 eV peak shift to higher binding energies, and peak width decreases even more due to the fall in intensity of species with $E_b < 530$ eV (Fig. 2b). Re-oxidation (spectrum not shown) produces a ≈0.5 eV peak shift to lower binding energies and FWHM increases slightly compared with the ion bombarded sample, and remaining less than sample as received. From Figs. 4a–c and Table 4, one can appreciate the difficulty of deducing the sample SLB1 as an Al_2O_3 and Fe_2O_3 mixture since, from the ratio N_{Al}/N_{Fe} there should exist 3.5 times more oxygen atoms bonded to aluminium than to iron and the O 1s peak should exhibit an asymmetry on the side of low binding energies.

The AT SLB1 sample in the as received (AR) condition exhibits a narrower O 1s peak (Fig. 2c) than the BT (oxidized) sample (Fig. 2a) with less contribution of species with $E_b < 530$ eV and $E_b > 532.5$ eV. This peak width decrease, despite the presence of a charge effect similar to that in the BT SLB1 sample, could indicate a sample surface chemical modification due to the catalytic test; ion bombardment of this sample produces a 0.3 eV shift to higher binding energies, without FWHM modification (spectrum not shown). Thermal treatment moves the binding energy peak value (Fig. 2d) to that obtained in the AT SLB1 sample as received (AR) and a slight width decrease because of reduction of species with $E_b > 532.5$ eV. Re-oxidation maintains the binding energy value, but the width decreases due to intensity reduction of species with $E_b > 532.5$ eV (Fig. 8g).

The comparison of the O 1s peaks for the BT SLB1 (not shown) and AT SLB1 (Fig. 8g) samples after re-oxidation shows that in the latter the peak width is appreciably narrower and with a ≈0.3 eV shift to lower binding energies. This shift is observed also in the Al 2p peak, such that the energy difference between the two is maintained (see Table 3); this can be attributed to charge effect correction problems rather than a chemical shift. Al 2p as a reference is more appropriate for this sample. If we conceive the sample surface as an oxide mixture and aluminate with different electrical conductivities and degrees of response to sample treatments, one could explain peak width changes and peak shifts observed with respect to C 1s of adventitious carbon in terms of differential charge effects; especially because annealing produces a width reduction, observed earlier [6] and is expected due to the relaxation caused by atomic vibrations.

Table 3
Kinetic energy differences E_k (Al 2p) − E_k (O 1s), E_k (Si 2p) − E_k (O 1s), E_k (O 1s) − E_k (Fe $2p_{3/2}$) for samples Al_2O_3, Fe_2O_3, Si O_2 and VL1 after several sample treatments

Sample	E_k (Al 2p) − E_k (O 1s)	E_k (Si 2p) − E_k (O 1s)	E_k (O 1s) − E_k (Fe$2p_{3/2}$)
Al_2O_3			
Calcined	456.7		
H_2 reduced	456.6		
Ion etched	456.7		
Re-oxidized	456.7		
Fe_2O_3			
AR			181
Calcined			181.1
Ion etched			181.1
H_2 reduced			180.3
Re-oxidized			180.6
SiO_2			
Calcined		428.9	
H_2 reduced		429.2	
Ion etched		429	
Re-oxidized		429.3	
VL1			
BT			
Oxidized	(*)456		(#)181.5
	(#)457.9		
Ion etched	(*)456.2		(#)181.0
	(#)457.8		
Annealed	(*)455.6		(#)180.6
	(#)457.1		
Re-oxidized	(*)456.2		(#)181.6
	(#)457.9		
AT			
AR	(*)456		(#)181.3
	(#)457.9		
Annealed	(*)455.7		(#)181.2
	(#)457.5		
Ion etched	(*)455.9		(#)180.8
	(#)457.7		
Re-oxidized	(*)456.2		(#)181.3
	(#)457.9		
SLB1			
BT			
Oxidized	(*)456.8		
Annealed	(*)456.9		
Ion etched	(*)456.8		
Re-oxidized	(*)456.9		
AT			
AR	(*)456.8		
Ion etched	(*)456.8		
Annealed	(*)456.8		
Re-oxidized	(*)456.8		
Mixture M			
AR	(†)456.6	(†)429.2	(†)180.9
Calcined	(†)456.4	(†)429.4	(†)180.9
H_2 reduced	(†)456.6	(†)429.4	(†)180.2
Re-oxidized	(†)457.5	(†)430.3	(†)179.8

(*) Values obtained using the apparent O 1s peak maximum. (#) Values obtained after the O 1s peak decomposition into the components related to Fe and Al. (†) Values obtained after the O 1s peak decomposition into the components related to Fe, Al and Si.

Table 4
Comparison of the surface atomic ratios obtained from XPS data, with the bulk atomic ratios

Surface ± 10%				Volume ± 10%		
Sample	N_{Al}/N_{Fe}	N_{Fe}/N_{Si}	N_{Al}/N_{Si}	N_{Al}/N_{Fe}	N_{Fe}/N_{Si}	N_{Al}/N_{Si}
SLB1				2.9	9.4	27.6
BT						
Oxidized	3.6					
Annealed	3.2					
Ion etched	3.0					
Re-oxidized	3.9					
AT						
AR	4.5					
Ion etched	3.9					
Annealed	4.2					
Re-oxidized	4.1					
VL1				1.7	22.9	38.0
BT						
Oxidized	0.9					
Ion etched	0.8					
Annnealed	0.9					
Re-oxidized	1.0					
AT						
AR	1.0					
Annealed	0.9					
Ion etched	0.9					
Re-oxidized	1.0					
Mixture M						
AR	1.1	0.8	0.9			
Calcined	1.1	0.8	0.9			
H_2 reduced	1.4	0.6	0.8			
Re-oxidized	1.0	0.9	0.9			

4.3. Comparison among samples: SLB1, Fe_2O_3, and Al_2O_3

The Fe 2p spectrum in the AR Fe_2O_3 sample (see Fig. 1e) is narrower than the SLB1 BT sample (oxidized) (see Fig. 1a) but show similar binding energy for the two Fe 2p levels. The Fe 2p region is broader in BT (oxidized) SLB1 than in the calcined Fe_2O_3 (not shown); and even broader than in sputtered Fe_2O_3 (spectrum not shown), with a well differentiated interpeak satellite. The Fe 2p spectrum for the re-oxidized BT SLB1 (not shown) is broader than in AR Fe_2O_3 (see Fig. 1e), with the interpeak satellite less pronounced; its width is very similar to re-oxidized Fe_2O_3 (Fig. 11h). The binding energy difference between the two spectra, could be real, or probably an artifact of a charge effect correction since in Fe_2O_3 the O 1s reference (530.3 eV) was used while the C 1s (285 eV) in SLB1. The same observations could be made when comparing the Fe 2p spectra of AT SLB1 re-oxidized (Fig. 11d) and re-oxidized Fe_2O_3 (Fig. 11h).

The O 1s spectrum of AT SLB1 (AR) (Fig. 2c) resembles, both in shape and width, that of calcined (Fig. 8b) and re-oxidized Al_2O_3 (not shown), except in binding energy where there is a difference; if Al 2p (74.6 eV) is used as binding energy reference for sample BT SLB1 as we did for Al_2O_3,

the binding energy difference disappears. This can be verified by calculating the kinetic energy difference, E_k (Al 2p) − E_k (O 1s), in each case (see Table 3); 456.7 eV is obtained for Al_2O_3 and 456.8 for AT re-oxidized SLB1 sample after correcting the kinetic energy, using the energy calibration of each spectrometer. A 456.9 eV value difference for re-oxidized sample BT SLB1 is obtained, and the O 1s peak is broader than in Al_2O_3.

5. Sample VL1

In Table 4, the ratios of the surface atomic concentrations obtained from our XPS data are compared with our calculated bulk atomic ratios obtained from the reported weight composition of this sample (11). An Al concentration decrease with respect the volume composition is observed. The Fe 2p, O 1s, and Al 2p XPS regions for the VL1 sample are presented in Figs. 5–7; a comparison between the Fe 2p region of VL1 (Fig. 5a–d) and Fe_2O_3 (Fig. 5e and f) is shown in Fig. 5; the O 1 s peak of oxidized BT VL1 is compared with Al_2O_3 (Fig. 4d) and Fe_2O_3 in Fig. 4. A comparison between the O 1s spectra of AT SLB1 (Fig. 8f and g), AT VL1 (Fig. 8d and e), Fe_2O_3 (Fig. 8c), Al_2O_3 (Fig. 8b), and SiO_2 (Fig. 8a) is shown in Fig. 8. For the VL1 sample, the C 1s line (285.0 eV) binding energy reference is used. The binding energies for this sample are given in Table 1.

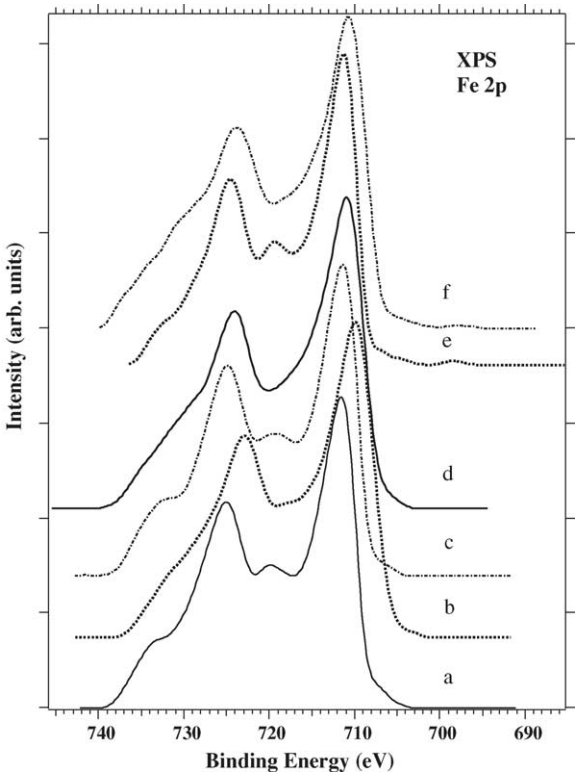

Fig. 5. The Fe 2p XPS spectra for sample VL1 after several sample treatments: (a) before catalytic tests (BT) and after an oxidation treatment; (b) BT after an Ar^+ ion etching and annealing treatments; (c) after catalytic tests (AT) in the as-received condition; (d) AT and after annealing and Ar^+ ion bombardment are compared to those of sample Fe_2O_3 after some sample treatments: (e) in the as-received condition; (f) H_2 reduction.

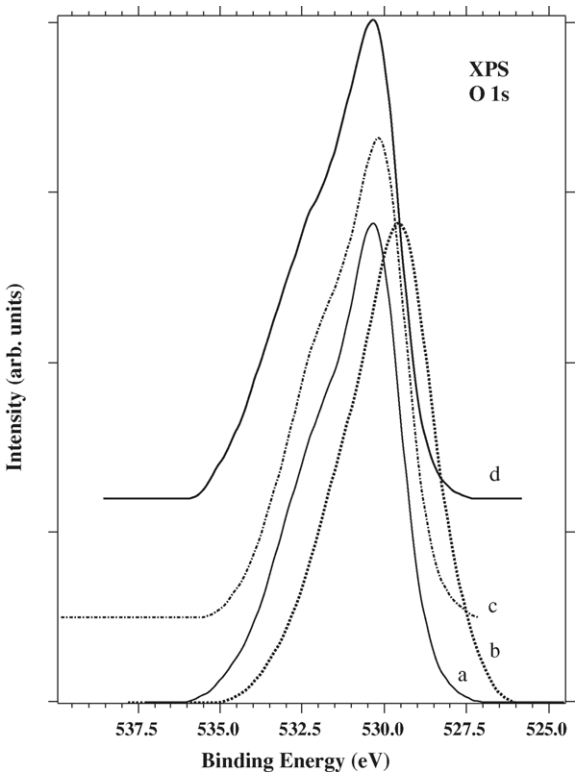

Fig. 6. The O 1s XPS spectral regions of sample VL1 in the following conditions: (a) before catalytic tests (BT) and after an oxidation treatment; (b) BT after an Ar^+ ion etching and annealing treatments; (c) after catalytic tests (AT) in the as-received condition; (d) AT and after annealing and Ar^+ ion bombardment are compared to those of sample Fe_2O_3 after some sample treatments: (e) in the as-received condition; (f) H_2 reduction.

A comparison of BT VL1 (Fig. 6a and b) and AT VL1 (Fig. 6c and d) is presented in Fig. 6. The Al 2p peak for the VL1 sample does not show appreciable changes except in AT VL1 at the state attained after heating and ion etching (see Fig. 7d) in which an increase of peak width is noticed; with re-oxidation the peak width exhibited in other treatments is recovered (not shown); Al 2p peak of BT VL1 (see Fig. 7a and b) did not show any changes after different treatments and are very similar to that obtained for sample AT VL1 (AR) (Fig. 7c) once the latter sample is exposed to ambient conditions. The observed difference in behaviour of AT VL1 (Fig. 7c and d) and BT VL1 indicates a modification in the chemical state of aluminum, as a result of the catalytic tests done with AT VL1.

5.1. Fe 2p level

The Fe 2p XPS spectrum of the BT VL1 sample after ion etching and annealing (Fig. 5b) exhibits a peak width increase, a shift to lower binding energies and a less definition of the interpeak satellite structure such as is expected from re-

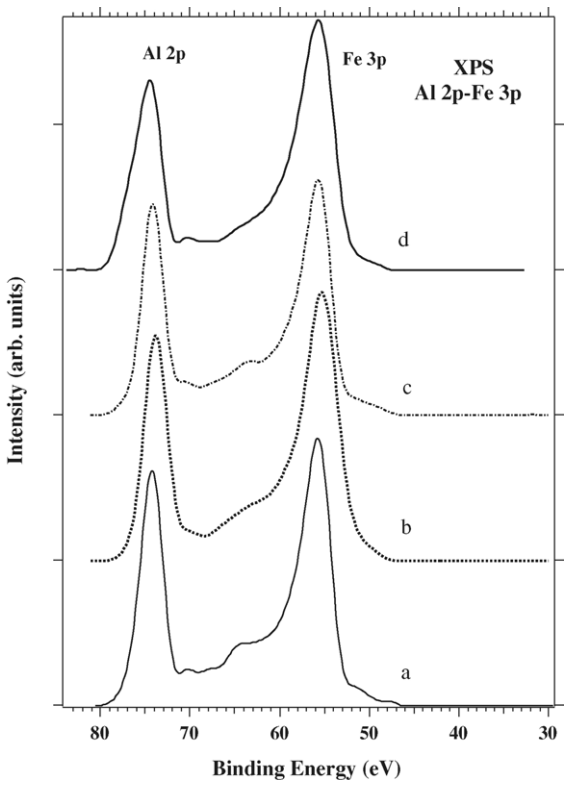

Fig. 7. The Al 2p XPS peak of sample VL1 for each of the sample conditions: (a) before catalytic tests (BT) and after an oxidation treatment; (b) BT after an Ar^+ ion etching and annealing treatments; (c) after catalytic tests (AT) in the as-received condition; (d) AT and after annealing and Ar^+ ion bombardment, is shown.

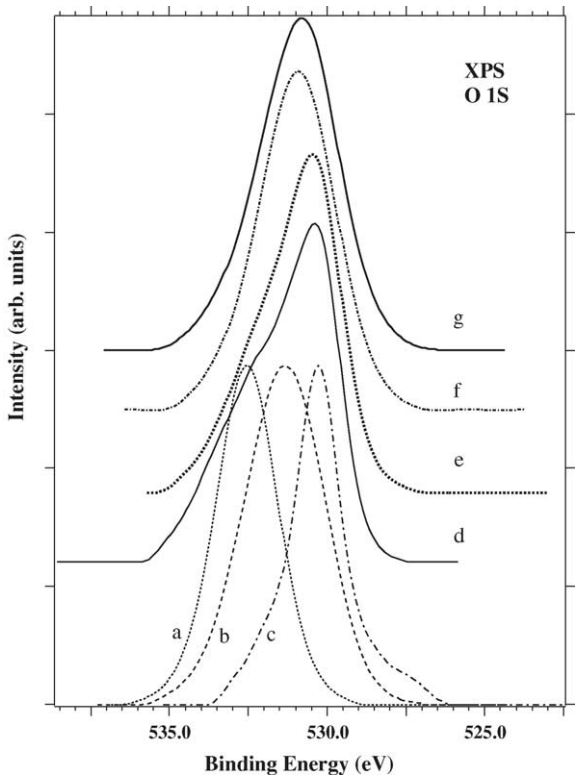

Fig. 8. A comparison of the O 1s peaks is shown for samples: (a) SiO_2 in the calcined condition; (b) calcined Al_2O_3; (c) calcined Fe_2O_3; (d) reduced AT VL1; (e) AT VL1 after a re-oxidation treatment; (f) reduced AT SLB1; (g) AT SLB1 after a re-oxidation treatment.

duced iron; re-oxidation (not shown) recovers the same XPS spectrum as that before these treatments. The AT (AR) VL1 spectrum (Fig. 5c) is similar to that of BT oxidized VL1. The AT VL1shows the same behaviour in the Fe 2p region (Fig. 5d), for the same sample treatments as BT VL1. Comparing this sample's Fe 2p spectra with Fe_2O_3, BT (oxidized) VL1 shows a Fe $2p_{3/2}$ peak (see Fig. 5a) slightly broader than AR Fe_2O_3 (see Fig. 5e) but similar to calcined Fe_2O_3 (not shown).

Ion etched BT VL1 exhibits a Fe $2p_{3/2}$ peak slightly broader than in ion etched Fe_2O_3; the Fe $2p_{3/2}$ peak shape (see Fig. 5b) of heated and ion etched BT VL1 resembles that of hydrogen reduced Fe_2O_3 (Fig. 5f), but there is a binding energy difference. The Fe 2p (not shown) of re-oxidized (BT) VL1 is similar to re-oxidized Fe_2O_3 (Fig. 11h) but with a 0.8 eV shift to higher binding energies. E_k (O 1s) − E_k (Fe $2p_{3/2}$) calculation for these two re-oxidized samples gives 180.6 eV for Fe_2O_3 and 181.6 eV for BT VL1. It could then be concluded that the Fe 2p spectrum in this sample resembles that of FeOOH, and its shape is very similar to AR Fe_2O_3 that before the calcination is closer to FeOOH [21]. AT (AR) VL1 has a Fe 2p spectrum similar to calcined Fe_2O_3 (not shown); in the same spectral region, heated and ion etched AT VL1 has a spectrum (see Fig. 5d) completely similar to hydrogen reduced Fe_2O_3 (Fig. 5f); comparison (Fig. 11b) of re-oxidized AT VL1 with Fe_2O_3 shows the same behaviour as sample BT VL1; in this case the E_k (O 1s) − E_k (Fe $2p_{3/2}$) difference is 181.3 eV.

5.2. O 1s level

The O 1s peak is always asymmetric at higher binding energies and shows appreciable changes after sample treatments, specially sample AT VL1. Re-oxidized BT VL1 (spectrum not shown) and AT VL1 (Fig. 8e) show the same O 1s spectrum. Comparing these spectra (Fig. 8) with those of Fe_2O_3 and Al_2O_3, the O 1s spectra of VL1 samples look like mixed spectra of these two oxides, but the intensity disagrees with the Al and Fe weight proportion present in this sample (see Table 4); according to the ratio N_{Al}/N_{Fe}, there should exist practically the same number of oxygen atoms bonded to Al than to Fe, this should produce an O 1s XPS peak with a slight asymmetry on the high binding energy side but without exhibiting the obvious structure observed in Fig. 4d and Fig.8d.

6. Mechanical mixture (MMLV5)

The Fe 2p and O 1s spectra for this sample, recorded with the VSW spectrometer, are presented in Figs. 9 and 10 (in

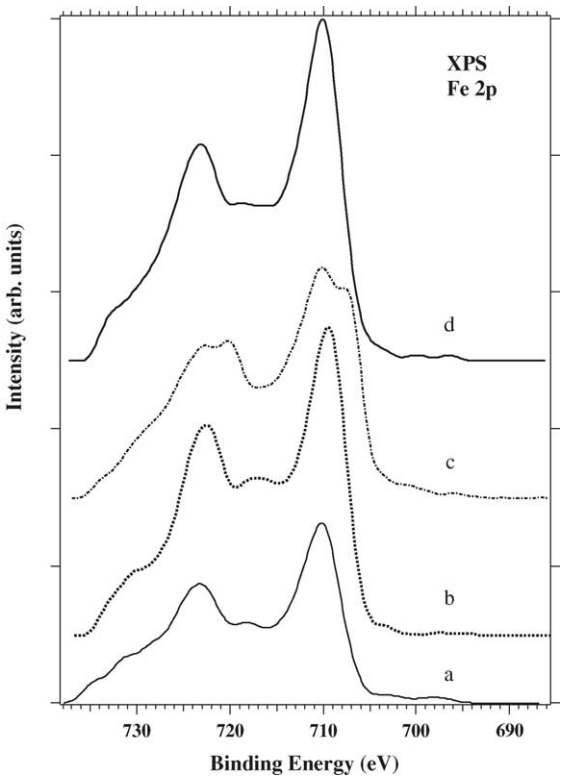

Fig. 9. The Fe 2p peaks for the mechanical mixture, (mixture M) analyzed in the VSW spectrometer after the following sample treatments: (a) in the as-received condition; (b) in the calcined condition; (c) after reduction in H_2; (d) after re-oxidation, are shown.

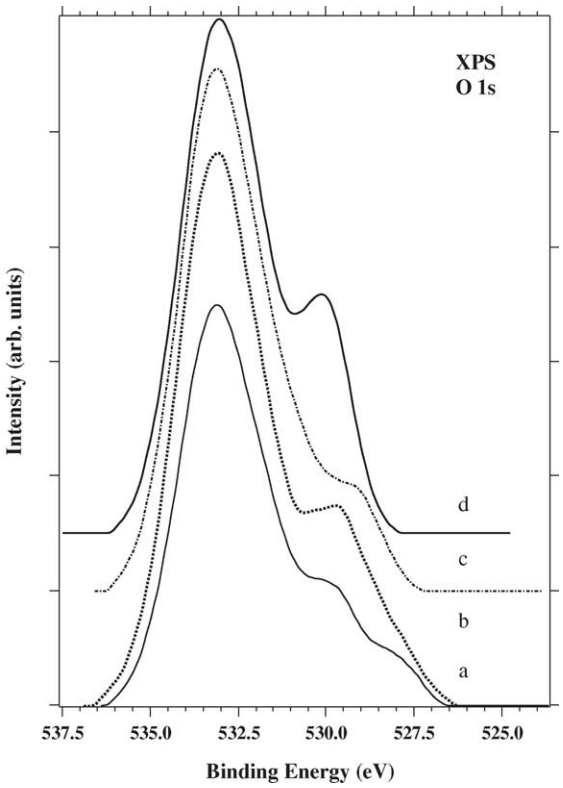

Fig. 10. The O 1s XPS spectral regions of mixture M under the sample treatments: (a) in the as-received condition; (b) in the calcined condition; (c) after reduction in H_2; (d) after re-oxidation, are presented.

this case, sample is named mixture M). A comparison of the Fe 2p regions in VL1, SLB1, mixture M and Fe_2O_3 is shown in Fig. 11. The values for the surface atomic concentration ratios for this sample are presented in Table 4. A Fe concentration decrease and a Al enrichment compared to Fe and Si is observed. The iron decrease is due to the sample deposition method that causes the heavier particles to stay away from the surface.

This sample, due to the heterogenous composition does not show an homogenous charge effect; however, the C 1s line (285.0 eV) was taken as a binding energy reference, despite the possible problems that could arise, but verifying whenever with the other internal energy references: Al 2p (74.6 eV) and Si 2p (103.8 eV). The XPS iron peaks cannot be used as references due to their susceptibility to several sample treatments, instead the O 1s bonded to iron (530.3 eV) was employed as reference to establish the presence of a differential charge effect in mixture M. This can be detected observing the Fe 2p, Si 2s and Al 2s binding energy values given in Table 2 for mixture M compared to those obtained for the pure oxides under the same sample treatments. The binding energies, taking the C 1s (285.0 eV) as binding energy reference, for this sample are given in Table 2.

The Fe 2p XPS spectrum (see Fig. 9a) for the AR mixture M sample exhibits a 0.7 eV binding energy shift compared with the calcined sample (Fig. 9b), which is the same as in Fe_2O_3; however, peak widths are larger than those in re-oxidized Fe_2O_3 and the interpeak satellite region is less defined (see Fig. 11f and h), which might be due to a differential charge effect arising from intergrain boundaries among the Fe_2O_3, Al_2O_3 and SiO_2 particles.

H_2 reduction for 20 h clearly shows (see Fig. 9c) a transformation to the metallic state of great part of the Fe_2O_3 content in the sample; the binding energy obtained for Fe 2p corresponds to that of metallic iron (Fe^0); re-oxidation (see Fig. 9d) recovers the calcined sample spectrum, but the interpeak satellite is less defined.

Evolution of O 1s component linked to iron (Fig. 10a–d) coincides with that observed in the Fe 2p region. The rest of the O 1s peak is practically, taking into account the weight composition (see samples section), related to oxygen bonded to silicon (SiO_2), which does not show modifications under sample treatments. Calculation of the E_k (Si 2p) $-$ E_k (O 1s) difference for SiO_2 and for the mixture M gives 429.2 ± 0.2 eV except for the re-oxidized mixture, which gives 430.3 eV. This variation could be due to a synergic effect that produces some sample chemical modification, thus departing from a mechanical mixture. Nevertheless, we should point out that the differential charge effect presence changes the O 1s peak shape where at least three components should exist. If the O 1s is decomposed using a peak fitting routine, errors can be committed when placing in position the differ-

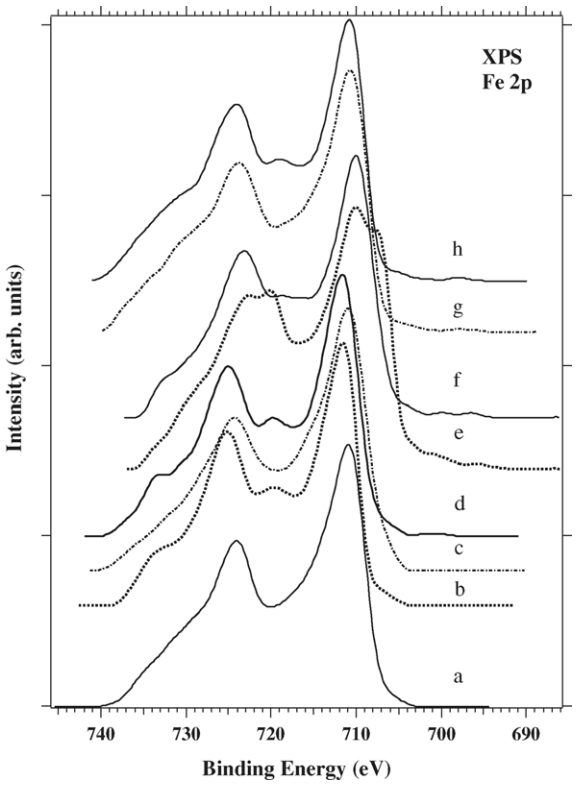

Fig. 11. The Fe 2p XPS spectral regions for several samples are presented: (a) reduced AT VL1; (b) re-oxidized AT VL1; (c) reduced AT SLB1; (d) re-oxidized AT SLB1; (e) mixture M reduced in H_2; (f) re-oxidized mixture M; (g) Fe_2O_3 reduced in H_2; (h) re-oxidized Fe_2O_3.

ent components since the fitting procedure is not univocal, leading to apparent values for the kinetic energy differences, which is not the case for the homogeneous charge effect.

Comparison of O 1s peak shape for the mechanical mixture (Fig. 10a–d) and that for VL1 (Fig. 6a–d) and SLB1 (Fig. 2a–d) shows that they are very different; in SLB1 the O 1s peaks are quite symmetrical, while in the mixture two oxygen species are clearly distinguished; in VL1 the peak asymmetry appears on the opposite site (left of peak maximum) to that observed in the mixture (right of peak maximum), despite that the surface atomic concentrations N_{Al}/N_{Fe} are not very different from those of VL1, and that the main difference between these samples is the ratio N_{Fe}/N_{Si} producing a contribution in the O 1s spectrum (mixture M) at 533.0 eV region due to oxygen bonded to Si.

7. Conclusions

The VL1 and SLB1 samples used as geologically standard reference laterites do not correspond at the surface to a mixture of oxides, but rather some type of iron aluminate present on their surfaces. These results confirm our former studies on not certified natural laterites.

The O 1s peak shape for the VL1 and SLB1 samples does not correspond to that expected if their surface composition were an oxide mixture in the proportion given by the N_{Al}/N_{Fe} ratios.

The mechanical Fe_2O_3, SiO_2 and Al_2O_3 mixture prepared to simulate a laterite exhibits a different behaviour to that observed on VL1 and SLB1 samples. This mixture shows a differential charge effect when it is irradiated with X-rays, which is not present on the standard reference laterites which supports the first conclusion.

It can also be concluded that in SLB1 sample the most appropriate internal binding energy reference is the 74.6 eV Al 2p level.

Acknowledgements

The authors like to thank Ecos-Nord and CONICIT for funding project ECOS V99, the authors are indebted to Dr. Labrecque for providing the geologically certified samples and to Dr. B. Fontal from the Department of Chemistry of ULA for reading the manuscript. J.M., R.C., F.R., and A.R. thank CDCHT-ULA for funding some of our research (project C-1130-02-05-AA) on oxides and we also thank Mr. J.C. Marchal and Mr. M. Clement from Laboratoire de Catalyse Hetérogène – Université de Lille I and Mr. J. Sarmiento from ULA for their technical assistance and cooperation.

References

[1] Maignen, Compte Rendu de Recherches sur les laterites, UNESCO, Paris, 1966.
[2] J.J. García, R.E. Galiasso, M.M. Ramirez de Agudelo, L. Rivas, J. Hurtado, US Patent 4701435 (1987).
[3] S. Yunes, D.S. Thakur, P. Grange, B. Delmon, Bull. Soc. Chim. Belg. 97 (1988) 84.
[4] F. Rueda, J. Mendialdua, Final report Project European Community CI1-0573-F(CD), 1994.
[5] G. Thornton, R. Casanova, Third year and final report. European Community on contract no. CI1-CI92-0056.
[6] F. Rueda, J. Mendialdua, A. Rodriguez, R. Casanova, Y. Barbaux, L. Gengembre, L. Jalowiecki, D. Bouqueniaux, J. Electron Spectrosc. Relat. Phenom. 70 (1995) 225.
[7] F. Rueda, J. Mendialdua, A. Rodriguez, R. Casanova, Y. Barbaux, L. Gengembre, L. Jalowiecki, D. Bouqueniaux, J. Electron Spectrosc. Relat. Phenom. 82 (1996) 135.
[8] F. Rueda, Doctoral Thesis, Université des Sciences et Tecnologies de Lille, France, 1997.
[9] M.M. Ramirez de Agudelo, B. Arias, J.J. García, N.P. Martinez, Rev. Tec. INTEVEP 10 (1990) 81.
[10] S. Yunez, A. Herbillon, P. Grange, B. Delmon, Bull. Soc. Chim. Belg. 97 (1988) 831.
[11] H. Schorim, J. LaBrecque, Geostandards Newslett. 7 (1983) 233.
[12] J. LaBrecque, H. Schorim, Fresenius J. Anal. Chem. 342 (1992) 306.
[13] Technical Report of ECOS-Nord project PI-99000235, 2001.
[14] J. Mendialdua, R. Casanova, J. Barbaux, J. Electron Spectrosc. Relat. Phenom. 71 (1995) 249.

[15] V.I. Nefedov, D. Gati, B.F. Dzhusinskii, N.P. Sergushin, V.S. Ya, Russ. J. Inorg. Chem. 20 (1975) 1279.
[16] T.L. Barr, VacF J., Sci. Technol. A 7 (1989) 1677.
[17] F. Rueda, J. Mendialdua, A. Rodriguez, R. Casanova, Y. Barbaux, L. Gengembre, L. Jalowiecki, D. Bouqueniaux, Surf. Interf. Anal. 21 (1994) 659.
[18] D.A. Shirley, Phys. Rev. B 5 (1972) 4709.
[19] J. Mendialdua, Ph D Thesis, number 559.Université de Sciences et Techniques de Lille, France, 1983.
[20] S. Hashimoto, K. Hirokawa, Y. Fukuda, K. Suzuki, T. Suzuki, N. Usuki, N. Gennai, S. Yoshida, M. Koda, H. Sezaki, H. Horie, A. Tanaka, T. Ohsubo, Surf. Interf. Anal. 18 (1992) 799.
[21] N.S. McIntyre, D.G. Zetaruk, Anal. Chem. 49 (1977) 1521.